Scholar Publishing Group
International Journal of Art Innovation and Development
https://doi.org/10.38007/IJAID.2020.010303
ISSN 2789-7192 Vol. 1, Issue 3: 28-44

Wear Resistance of Nano Surface Modified Layer Based on Powder Metallurgy Parts in Stone Carving Design

Yafei Mi*

Luxun Academy of Fine Arts, Shenyang, Liaoning, 110000, China

**corresponding author*

Keywords: Powder Metallurgy, Nano Surface Modification Layer, Abrasion Resistance, Stone Carving Design

Abstract: With the progress of time and the development of art, stone carvings are no longer simply dressing and embellishment of the environment. Instead, it has become an art form that embodies the consciousness of human creation, seeks the expansion and flow of space, gives people appreciation and participation from all-round or multiple angles, and has certain recreational or entertainment purposes. This article aims to explore the application of the wear resistance of the nano surface modified layer of powder metallurgy parts in stone carving design. This article first analyzes the wear mechanism of the material, proposes a numerical solution method for the nano-motion equation of powder metallurgy parts, and then explores the influence of SiO2 nanomaterials on the wear resistance and corrosion resistance of the composite coating. At the same time, the friction loss performance of nanomaterials of powder metallurgy parts is explored, and the adsorption rate of heavy metal ions is studied based on nanometer surface modification of powder metallurgy parts, and then the garden stone carving design based on nanomaterials is explored. The experimental results in this paper show that when the concentration of Cu2+ solution ranges from 1 mg/L to 3 mg/L, the removal rate of nanotubes after modification is increased by up to 11% compared with that before modification; When the concentration range of Zn2+ solution is 1mg/L~5mg/L, the removal rate of nanotubes after modification is increased by up to 20% compared with that before modification. At the same time, the stone sculptures based on the nanometer design of powder metallurgy parts also have good wear resistance.

1. Introduction

When the human society was in its infancy, it was known that tools were made by knocking stones, which produced aesthetic awareness and began to make artistic decorations. Carved patterns attached to practical objects and stone sculptures that purely reflected life also began to appear. The simple and straightforward beauty shown in these artistic relics is in the same line as the stone

carvings of later generations. In the historical development, some traditional stone carving production areas have emerged, often close to the mountainous area, and the artists have also passed on the materials from generation to generation. For example, Quyang, Hebei, has Huangshan Mountain and is rich in marble. It is an ideal stone carving material. Since the Han Dynasty, some people have been engaged in stone carving. In addition, Shoushan in Fujian and Qingtian in Zhejiang also used local materials to sculpt small desk stone carvings, seals, and seals. Quyang stone carvings generally pay more attention to the overall effect. The shape is simple and rough, vigorous and simple, and sometimes exaggeration is used to make the image more vivid and touching, which has a surprisingly winning effect. There are different styles in different places, with various poses, dynamic or quiet, lively and steady, with moving artistic charm.

Stone carving, as the name suggests, is a form of carving. It is a kind of art that creates a spatial image by means of carving, carving, grinding, cutting, etc. The materials used are also limited to stone. Stone is the oldest sculptural material used by humans. Some people vividly refer to history as being made of stone and bronze. It has the characteristics of long-term preservation and weathering resistance. It can produce rich textures, and it is the first choice for historical figures representing major themes and large volumes. This article explores the application of the wear resistance of the nanometer surface modification layer of powder metallurgy parts in the design of stone carving, which has positive significance for improving the level of stone carving art and protecting the ancient handcraft of stone carving.

According to the research progress at home and abroad, different scholars have also made certain researches on the wear resistance of the nano-surface modified layer and the design of stone carvings: Brzhozovskii B M obtained an analytical model for calculating the working life of cutting tools with a plasma-modified surface layer. It allows to calculate the conditions to ensure the improvement of tool wear resistance, thereby improving the reliability of CNC machine tool manufacturing [1]. Stepankin I N introduced the experimental results of X165GrMoV12 and X160GrMoV12-1 steels under pulsating load under contact wear. The difference in wear resistance of the surface layer is related to the synthetic mode of its structure and performance. The structure evolution characteristics of the nitrocarburizing hardened modified layer are revealed. Determine the thermochemical treatment mode aimed at achieving maximum resistance to pulsating contact stress [2]. Ivanov Y F studied the formation of nano-structured multi-phase surface layers in high chromium 12X18H10T and 20X13 stainless steel under the action of strong pulsed electron beams in the SOLO system. The Fe-Cr-C system has been thermodynamically analyzed. Alloying Fe-Cr alloy with carbon will significantly change its structure and phase state, and determine the existence area of carbides M23C6, M7C3, M3C2 and M3C with α and γ phases [3]. Tsyganov V V takes into account the wear of the steel parts of the friction coupler under dynamic loading. Note the relationship between the wear resistance of the metal and the structural uniformity of the surface layer. A model of surface structure failure during friction under single-component, double-component and three-component dynamic loads is proposed. The principle of surface engineering and the algorithm of controlling the wear resistance of steel by using the characteristics formed by the nanostructure state of the surface layer are analyzed [4]. Wang Z G aims to provide basic insights into the grain size dependence and mechanical behavior of hot-pressed Al2O3-ZrO2 ceramics under its eutectic composition, and to further explore the hardening effect of laser-induced surface nano-eutectic layers. The potential correlation between densification behavior, grain size distribution and mechanical properties is clarified. Sintering at 1550℃ promotes densification without extensive grain growth. In this case, the critical density of the sample is 99.3%. It provides a broad prospect for the application of sliding ceramic parts to significantly improve the hardness and wear resistance [5]. After Zagulyaev D V used a pulsed electron beam with a specific energy of 35J/cm2 to perform electron beam treatment on AK10M2N silicon and aluminum, the

microhardness of the surface layer increased from 0.99GPa to 1.18GPa. At the same time, the friction coefficient reduces the wear coefficient by 1.3 times, and the wear coefficient is 6.6 times. It has been found that the changes in the mechanical and tribological properties of the silicon-aluminum surface layer are related to significant structural transformations, such as the dissolution of silicon and intermetallic compounds during the irradiation of the material with a high-intensity pulsed electron beam [6]. Potekaev AI introduced the research results of phase and element composition, defect substructure state, mechanical and tribological properties of the modified surface of steel Gr1The modification process includes plasma spraying of Ni-Cr-B-Si-based powder coating, followed by high-intensity pulsed electron beam irradiation. The results show that the surface of the coating formed by plasma spraying contains micropores and macropores, and has the characteristics of high relief [7]. However, these scholars did not combine the wear resistance of the nano-surface modified layer with the stone carving design to discuss the problem, but only unilaterally explored their significance.

The innovations of this paper are mainly reflected in: (1) Analyze the wear mechanism of materials, and propose a numerical solution method for the nano-motion equation of powder metallurgy parts; (2) The influence of SiO2 nanomaterials on the wear resistance and corrosion resistance of composite coatings was explored, and the friction loss properties of nanomaterials for powder metallurgy parts were explored at the same time. And based on the nano-surface modification of powder metallurgy parts, the adsorption rate of heavy metal ions was studied, and then the design of garden stone carving based on nano-materials was explored.

2. Application Method Based on the Wear Resistance of the Nano Surface Modified Layer of Powder Metallurgy Parts in Stone Carving Design

2.1. Material Wear Mechanism

When objects contact and move relative to each other, damage to the surface materials of the objects occurs when they move with each other. This process is called abrasion. Studies have shown that there are three main forms of wear of mechanical parts: wear, fracture and corrosion, accounting for about 60%-80%. The damage caused by wear is shocking, and the issue of wear has attracted much attention [8]. Studying the wear mechanism of materials and improving the wear resistance of materials can effectively save materials and energy, improve the applicability of parts and machines, and extend their service life. As shown in Figure 1, the structure of nanomaterials [9].

According to the function of the surface, the change of the friction surface and the destruction of the material, the wear can be divided into abrasive wear, adhesive wear, fatigue wear and other forms of wear [10].

(1) Abrasive abrasive wear

The surface of the object has roughness and hard protrusions; the mutual friction between the surface of the object, the surface solid particles or solid protrusions, are easy to peel off and cause the reduction of the surface material of the object. This phenomenon is called abrasive wear [11]. Among the different forms of material wear, about 50% of the wear is caused by abrasive wear, which is a very dangerous and serious form of material wear. The surface hardness and hardness difference of the friction pair are the main factors affecting wear [12]. The wear of metals and various crude steel materials is proportional to their hardness, and the wear depends on the size and shape of the mill [13].

(2) Adhesive abrasion

The actual contact area between the two parts of the friction is only a small part of the surface contact area, making the material surface in a plastic state; When the friction surfaces slide relative

to each other, shear will be generated due to the adhesion effect. The fracture of the material can be removed from the surface of the material, or it can be transferred from the surface of the material to the surface of another material, which is called viscous wear. Factors such as the inherent properties of the material, load and speed affect the viscous wear of the material [14].

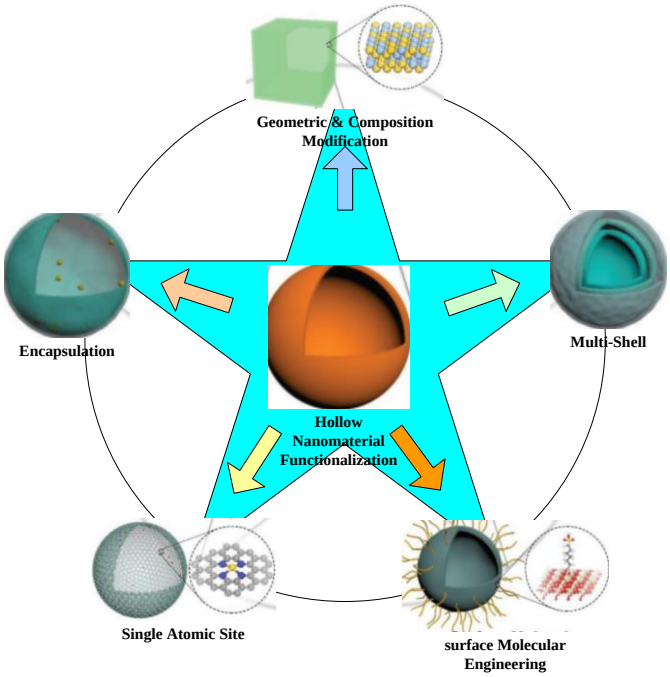

Figure 1. Structure of nanomaterials

(3) Fatigue wear

When relative rolling or friction is accompanied by relative sliding, the surface of the material is prone to fatigue wear; under certain sliding friction, the material will also experience fatigue wear. The failure principle of fatigue wear is to rub the surface under the action of variable contact pressure, and the material surface will fall off due to fatigue damage [15].

(4) Other forms of wear

Other forms of wear include erosion, corrosion, impact and microdynamic wear. When the surface of the material is affected by small and loose particles, the surface of the material will be destroyed, which is called abrasive wear [16]. When the surface and the surface slide relative to each other, if the surface material reacts with the environment, the surface material will be lost under mechanical action. This phenomenon is called corrosion wear [17]. If there are small fluctuations between the surfaces of the double-sided pressed material, the material is prone to complex wear, which is called micro-dynamic wear. Impact wear is a special wear method, and it is also the wear method of three-body abrasives under a moving load [18].

2.2. Numerical Solution Method of Nano-Motion Equation of Powder Metallurgy Parts

In order to study the dynamics of nanodevices, we use numerical calculation methods and consider linear damped oscillators. The energy dissipation of the vibrator causes the amplitude of the vibrator to decrease with time [19]. Therefore, in order to maintain the stable vibration of the graphite vibrator, it is necessary to supplement energy to the vibrator. We assume that the dissipation can be compensated by the applied periodic harmonic force. If the Langevin random force and the disturbance of the graphite sheet are ignored, the oscillator dynamics equation can be described as:

$$er = -\partial W(a) - \vartheta b + Q_n \sin(\beta d + \delta) \quad (1)$$

Where e is the mass of the movable top graphite sheet, a and b are the displacement and velocity of the top layer relative to the fixed bottom graphite sheet, and Q_n is the amplitude of the driving force applied to the top layer with angular frequency β and initial phase δ, ϑ is the coefficient of friction, with a value of 0.1.

It can always be $J(a,b) = \frac{1}{2}b^2 + W(a)$. You can get after points

$$a(d) - a(0) = \int_0^d b(d)dt \quad (2)$$

$$b(d) - b(0) = \int_0^d [-\partial W(a)]dt - \vartheta \int_0^d b(d)dt + \int_0^d [Q_n \sin(\beta d + \delta)]\, dt \quad (3)$$

We assume that the initial velocity is equal to zero. In order to obtain stable vibration, the motion state of the vibrator and the driving force must be the same as the original motion state after a period D [20]. Therefore, the angular frequency β of the driving force must be equal to an integer multiple of the eigenfrequency f [21].

$$\beta = nf \quad (4)$$

Although frequency is only a small set of all possible frequencies, the above formula is indispensable. Limiting the solution of this set is not artificial. Outside of this set, the oscillator system cannot always recover completely after one cycle [22].

In order to ensure that the non-harmonic oscillator and the external driving force are completely restored in one cycle, the displacement, velocity and energy have strict periodicity. Once the external driving force is given, its period cannot be changed [23]. So the vibrator must adjust its parameters, such as displacement and phase, in order to match the vibrator's frequency with the driving frequency [24].

For any given initial condition, in the presence of dissipation and external drive, after one round-trip oscillation, its maximum displacement will be the initial condition of the next oscillation. If the initial conditions are right, in a cycle, the energy $K_{in}(a_i, Q_n, \theta) = Q_n \int_0^D \sin(mfd + \theta) b(d)dt$ provided by the external driving force is exactly equal to the dissipation energy $K_{out}(a_i, Q_n, \theta) = -\int_0^D \vartheta b^2(d)dt$ caused by friction, and stable vibration can be maintained, thus:

$$\int_0^D \{Q_n \sin(mfd + \theta) - \vartheta l(d)\} l(d)dt = 0 \quad (5)$$

However, this condition only satisfies the energy condition, and does not guarantee that the displacement and velocity will return to the initial value at the same time after a period of time [25]. The displacement at time d depends on many factors, including the shape of the potential, the initial displacement, the coefficient of friction, and the frequency, initial phase, and amplitude of the driving force. In order to maintain stable vibration, the displacement and velocity must return to the initial value within a period D. They satisfy the relation:

$$a[d = D; W(a), a(0), \vartheta, \beta, \delta, Q_n] = a(0) \quad (6)$$

$$l[d = D; W(a), a(0), \vartheta, \beta, \delta, Q_n] = l(0) \quad (7)$$

It is very difficult to completely determine these two conditions involving multiple parameters. If the driving frequency satisfies the formula (4), the conditions for stable vibration are determined by the initial phase and amplitude of the control force. Each simultaneous equation gives a curve of solution in the $\delta - Q_n$ plane. The intersection of the two curves gives their simultaneous solution.

There are several branches of algorithms for numerically solving particle motion states, including Leap-frog, Gear, BeemanVerlet and Velocity-Verlet. They have their own advantages.

The starting point is to expand the position, velocity and acceleration of the particles according to Taylor series.

The disadvantage of the Leap-frog algorithm is that the velocity and position are not defined at the same time, so the trajectory of the particle and the total energy of the system cannot be calculated at the same time. The stability of the Gear algorithm is not very good, the calculated energy changes greatly, and it requires more memory and time than the Verlet algorithm. The advantage of the Verlet algorithm is its high numerical stability. The more entangled thing is that the accuracy of calculating the position and velocity of the particles is different.

In practice, the Velocity-Verlet algorithm is more widely used. It can obtain position, velocity, and acceleration at the same time, and is easy to program, requires less memory, has high stability, and does not sacrifice accuracy.

Using the Verlet algorithm to simulate the need to know the position, velocity and acceleration of the particles at the first time d. The following formula shows how the Verlet algorithm calculates the position and velocity at time $d + \Delta d$:

$$\bar{a}(d + \Delta d) = \bar{a}(d) + \bar{l}(d)\Delta d + \frac{1}{2}\bar{k}(d)\Delta d^2 \tag{8}$$

$$\bar{l}(d + \Delta d) = \bar{l}(d) + \frac{\bar{k}(d)+\bar{k}(d+\Delta d)}{2}\Delta d \tag{9}$$

Where Δd is the time step? It can be seen that after an integration step, the state is advanced one time step forward. Therefore, the Velocity-Verlet algorithm can be used to solve the nano-motion equation of powder metallurgy parts.

3. Application Experiment Results Based on the Wear Resistance of the Nano Surface Modified Layer of Powder Metallurgy Parts in the Design of Stone Carvings

3.1. Influence of SiO2 Nanomaterials on the Wear Resistance and Corrosion Resistance of Composite Coatings

The superhydrophobic material with static contact angle greater than 150 °and rolling angle less than 10 °, used on the surface of light alloy, can not only improve the self-cleaning ability and anti-icing ability of aluminum alloy, but also improve the corrosion resistance of aluminum alloy. Therefore, the study of wear-resistant and corrosion-resistant superhydrophobic coatings on aluminum alloy surfaces has received extensive attention. However, to make the surface super-hydrophobic, two conditions must be met at the same time: (1) Designing micro-nano rough structure on the super-hydrophobic surface; (2) Reduce the surface energy of the micro-nano rough structure. Studies have shown that super-hydrophobic coatings are easily scratched and scratched by small particles, leading to damage to its micro-nano structure and loss of super-hydrophobic properties. Therefore, the preparation of wear-resistant superhydrophobic materials is a difficult point and an important problem to be solved urgently. However, adding hard SiO2 particles to the surface of superhydrophobic materials can enhance the wear resistance of superhydrophobic coatings. Therefore, it is very important to study the influence of SiO2 content on the wear resistance and corrosion resistance of superhydrophobic coatings.

Figure 2 shows the relationship between the contact angle of the water droplet and its surface measured after sliding 2m, 4m, 6m, and 8m when the PPS-PTFE/SiO2 composite coating is loaded on 800 mesh SiC sandpaper with a load of 1N. It can be seen from the figure that the contact angle of the PPS-PTFE coating has a downward trend after the sliding friction distance is 2m, 4m, 6m, and 8m. After 8m of sliding friction, the contact angle of the PPS-PTFE coating decreased by approximately 3 °, and the decrease in the contact angle was very small. This is because the PPS as

the matrix has excellent adhesion properties, which enables the PPS-PTFE coating to adhere tightly to the surface of the aluminum alloy substrate, avoiding damage to the PPS-PTFE coating due to load friction. In addition, PPS has excellent mechanical strength and can reduce the damage caused by friction. In addition to the contribution of PPS, PTFE plays a lubricating role during the sliding process due to its small friction coefficient, which helps to reduce friction and wear. Therefore, the contact angle of the PPS-PTFE coating does not change much after 8 m of sliding friction.

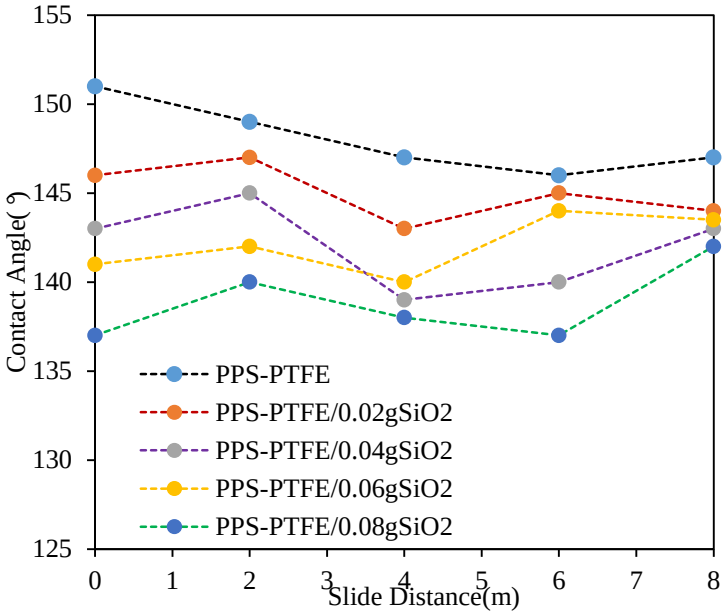

Figure 2. The influence of sliding distance on contact angle

After adding SiO2 to the coating, the contact angle of the PPS-PTFE/SiO2 composite coating did not increase or decrease significantly after sliding friction of 2m, 4m, 6m, 8m. The reason may be that SiO2 is a kind of hard particle, which has a great hardness. After being added to the coating, the hardness of the coating is increased, and the wear of the coating after friction is reduced. In addition, the particle size of PPS and PTFE is much larger than that of SiO2. After friction, the SiO2 particles leave their original positions and are distributed in the coating, which changes the morphology of the coating. SiO2 is a nanometer particle, which can modify the rough morphology of the coating to a certain extent. The above results show that the addition of SiO2 nanoparticles is beneficial to improve the wear resistance of the coating.

In a 3.5wt.% NaCl solution, the Tafel curves of five coating samples and aluminum alloy substrates were tested, and the corrosion resistance of the coatings was analyzed. As we all know, the corrosion potential can detect the ease of corrosion of the sample. The higher the corrosion potential, the more difficult it is for the sample to be corroded and the better the corrosion resistance. The corrosion current density refers to the corrosion speed of the sample. The lower the corrosion current density, the slower the corrosion rate of the sample and the better the corrosion resistance.

It can be seen from Table 1 that the corrosion potential of the aluminum alloy substrate is -1.079V. The corrosion potentials of five samples of PPS-PTFE/SiO2 composite coating ranged from -0.603V to -0.495V. Compared with the corrosion potential of the aluminum alloy substrate, the corrosion potential of the five samples of the PPS-PTFE/SiO2 composite coating showed a significant positive shift, suggesting that it has a lower tendency to be corroded. In addition, the corrosion current density of the PPS-PTFE/SiO2 composite coating is lower than the corrosion current density of the aluminum alloy substrate, which is 3.601*10-5A/cm2, which implies that its

corrosion rate is lower. The PPS-PTFE/SiO2 hydrophobic coating effectively protects the aluminum alloy substrate and improves its corrosion resistance. The main reason is that the super hydrophobic coating effectively isolates the aluminum alloy substrate from contact with the electrolyte, thereby protecting the aluminum alloy substrate; Because of the chemical inertness of PPS and PTFE, it is difficult for chemical reactions to occur, and the coating is made to protect the aluminum alloy substrate to a large extent. In addition, the influence of SiO2 content on the corrosion resistance of PPS-PTFE/SiO2 composite coating has no obvious law.

Table 1. Corrosion potential and corrosion current density of PPS-PTFE/SiO2 composite coating with different SiO2 content

Samples	Ecorr(V)	Icorr(A/cm^2)
Al alloy substrate	-1.079	$3.601*10^{-5}$
PPS-PTFE	-0.602	$2.003*10^{-5}$
PPS-PTFE/0.02gSiO_2	-0.603	$2.604*10^{-5}$
PPS-PTFE/0.04gSiO_2	-0.497	$3.571*10^{-5}$
PPS-PTFE/0.06gSiO_2	-0.495	$2.599*10^{-5}$
PPS-PTFE/0.08gSiO_2	-0.518	$2.641*10^{-5}$

3.2. Friction Loss Properties of Nanomaterials in Powder Metallurgy Parts

The sample of Fe-5Cr-lMo-0.9Si-2.4C-0.6P composition was subjected to oil lubrication friction and wear test on the MR-H5 ring block high-speed friction and wear tester, and the hardness of the material was 52HRC. The test speed is 500r/min, and the test loads are respectively 300N, 500N, 700N, 900N. The change curve of the friction coefficient with time under different loads after abrasion is shown in Figure 3.

When the load is 300N, the friction coefficient rapidly increased to the maximum value of 0.12 at the beginning of the test and decreased to 0.16 in a short period of time; then the friction coefficient increased to 0.18 again, and then gradually decreased to 0.14 and remained stable; the running-in period is the shortest, about 240s. When the load is 500N, the friction coefficient rapidly increased to the maximum value of 0.095 at the beginning of the test and decreased to 0.083 in a short time; then the friction coefficient increased again to 0.085 and decreased to 0.08 at about 700s; After that, the friction coefficient increased to 0.082 around 750s and fluctuated up and down at this value; the running-in period was longer than 300N, which was 750s. When the load is 700N, there is a large fluctuation in the friction coefficient at the beginning of the test. First increase to 0.08 and

then decrease to 0.075, increase to the maximum value of 0.085 at 250s, and maintain a decreasing trend between 250s and 750s. Afterwards, between 750s and 1250s, it increased from 0.082 to 0.084 and remained stable; its running-in period was 1250s. When the load increases to 900N, the friction coefficient first increases to 0.098 and decreases to 0.082 in a short time; After that, it maintained an upward trend and reached the maximum value of 0.10 at 250s; between 250s and 750s, the friction coefficient showed a decreasing trend, and was 0.082 at 750s; Between 750s and 1400s, the friction coefficient shows an increasing trend, and at 1400s it is 0.085 and remains stable. In summary, as the load increases from 300N to 900N, the running-in period of the material gradually increases; when the load is low, the powder metallurgy material can quickly enter the stable wear stage.

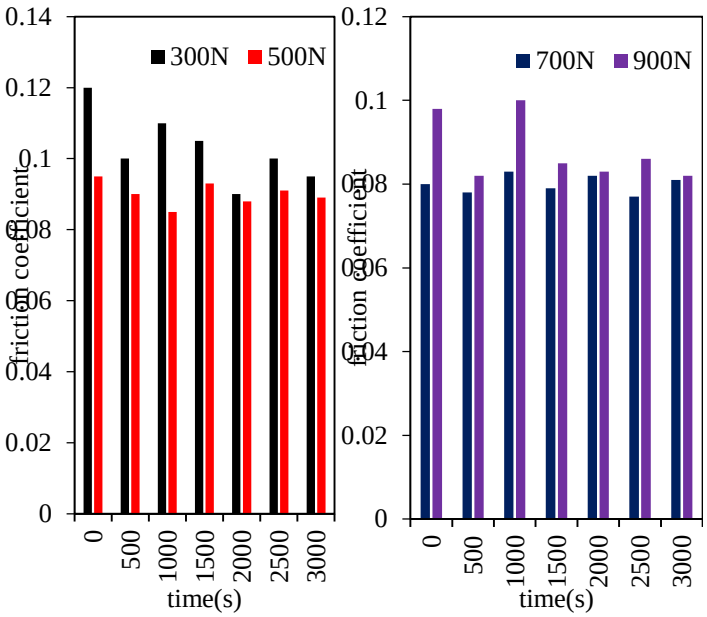

Figure 3. Friction coefficient-time diagram under different loads

Choose the above test load to be 500N, and the test speed to be 500r/min, 1000r/min, 1500r/min, 2000r/min. At different speeds, the friction coefficient changes with time as shown in Figure 4.

When the speed is 500r/min, the friction coefficient at the beginning of the test rapidly increases to the highest point of 0.12 and then rapidly decreases, and it is 0.11 at 30s; The friction coefficient keeps increasing trend between 30s~100s, and it is 0.115 at 100s; the friction coefficient between 100s~200s gradually decreases to 0.102; after 200s, the friction coefficient gradually decreases with the increase of time; the running-in period is 200s. When the speed is 1000r/min, the friction coefficient at the beginning of the test rapidly increases to 0.105 and then rapidly decreases to 0.10; after 35s, the friction coefficient keeps increasing, and it is 0.115 at 300s; After 300s, the friction coefficient tends to increase slowly with the increase of time, and there is a big fluctuation at 2900s; the running-in period is 300s. When the speed is 1500r/min, the friction coefficient gradually increases to 0.09 between 0 and 500s, and the friction coefficient fluctuates around 0.09 after 500s; the running-in period is 500s. When the speed is 2000r/min, the friction coefficient gradually increases to 0.09 between 0 and 550s, and decreases to 0.08 between 550s and 650s. After 650s, the friction coefficient remains basically stable; the running-in period is 650s. In summary, as the speed increases from 500r/min to 2000r/min, the running-in period of the material gradually increases.

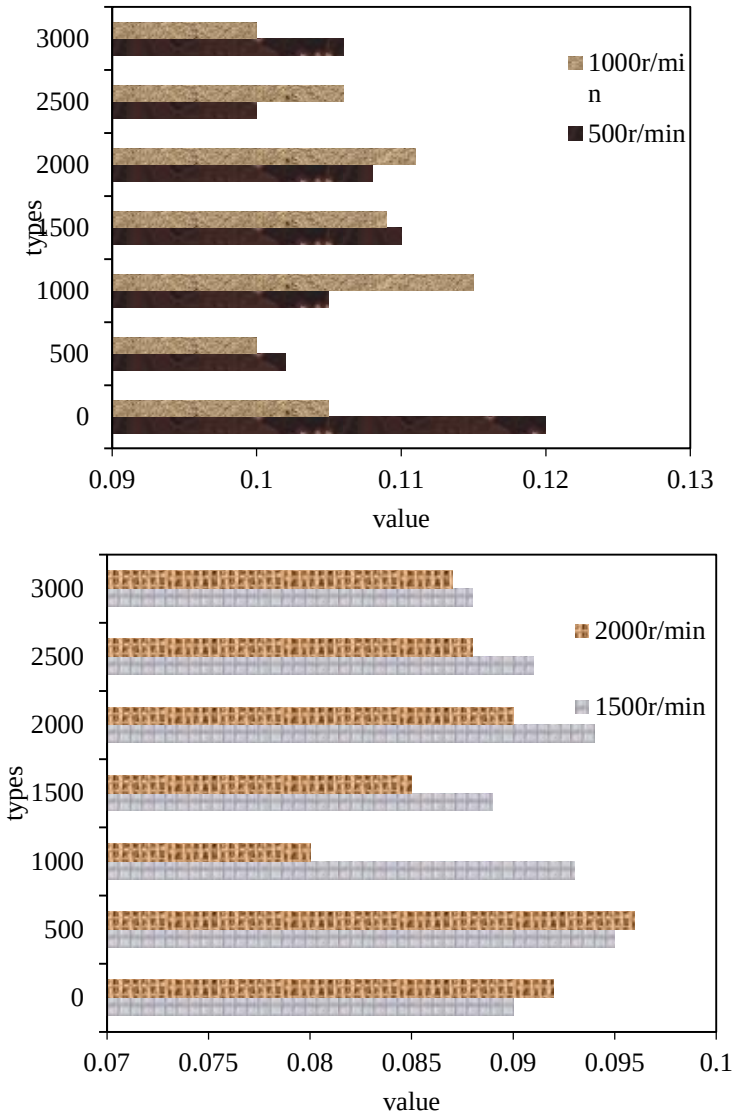

Figure 4. Friction coefficient-time diagram at different speeds

3.3. Adsorption Rate of Heavy Metal Ions by Nano-Surface Modification of Powder Metallurgy Parts

The nanotubes of the powder metallurgy part before and after the modification adsorbed Cu2+ and Zn2+ in the solution respectively. The following is the result of the adsorption time relationship of the nanotubes before and after the modification.

(1) Experimental data of Cu2+ removal by nanotubes before and after modification in different adsorption times

At room temperature, take 100ml of Cu2+ solution with a concentration of 1mg/L and a pH of 6, add 10mg of adsorbent, and shake with a constant temperature oscillator at a speed of 150r/min for 20min, 40min, 60min, 80min, filter this solution and take the clear solution to determine the concentration after adsorption. The adsorption results of nanotubes before and after modification are shown in Table 2 and Table 3.

Table 2. The relationship between nanotube adsorption of Cu2+ and time before modification

Time (min)	Absorbance	The amount of Cu^{2+} (ug)	Cu^{2+} initial concentration (mg/L)	Concentration of Cu^{2+} (mg/L)	Adsorption capacity	Heavy metal ion removal rate
20	0.149	9.1231	1	0.9632	0.3021	2.8732
40	0.137	8.9872	1	0.8971	0.8502	9.8967
60	0.135	8.5921	1	0.8534	1.2732	12.7963
80	0.135	8.5921	1	0.8534	1.2732	12.7963

Table 3. The relationship between adsorption of Cu2+ by nanotubes and time after modification

Time (min)	Absorbance	The amount of Cu^{2+} (ug)	Cu^{2+} initial concentration (mg/L)	Concentration of Cu^{2+} (mg/L)	Adsorption capacity	Heavy metal ion removal rate
20	0.139	8.721	1	0.9231	0.6332	5.9832
40	0.129	7.8932	1	0.8121	1.2315	20.0983
60	0.118	7.1982	1	0.7123	2.3812	23.8965
80	0.118	7.1982	1	0.7123	2.3812	23.8965

It can be seen from the above table that the adsorption capacity of nanotubes before and after modification increases with the increase of adsorption time. When the adsorption time is 80 minutes, the adsorption capacity of nanotubes before modification is 1.27 mg/g, and the adsorption capacity of nanotubes after modification is 2.38 mg/g. The relationship between the removal rate and the adsorption time is shown in Figure 5 (left) below.

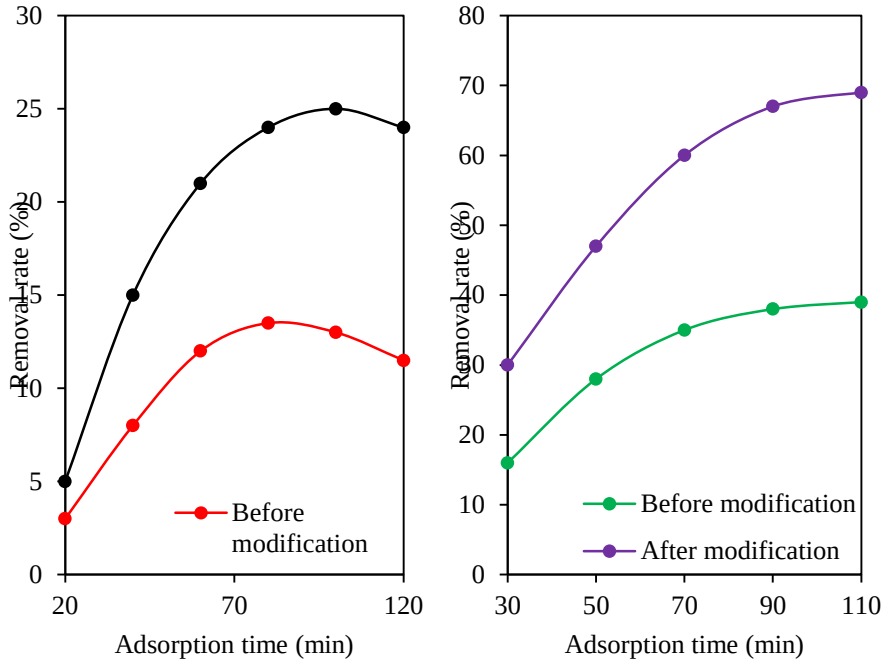

Figure 5. The relationship between the removal rate of Cu2+ and Zn2+ by nanotubes before and after modification and time

It can be seen from the results in the figure that the removal rate of Cu2+ by carbon nanotubes before and after modification increases with the increase of adsorption time. The time for the adsorption to reach equilibrium is 90 minutes, and the removal rate of nanotubes before and after the modification is 14% and 26% respectively; The adsorption time is within 30min-60min, and the adsorption rate of carbon nanotubes to Cu2+ is very fast before and after modification. At this time, the removal rate of nanotubes after modification is up to 12% higher than that before modification.

(2) Experimental data of Zn2+ removal by nanotubes before and after modification in different adsorption times

At room temperature, take 100mL of Zn2+ solution with a concentration of 3mg/L and pH of 2.5, add 20mg of adsorbent, and shake with a constant temperature oscillator at a speed of 150r/min for 20min, 40min, 60min, 800min, filter this solution and take the clear solution to determine the concentration after adsorption. The adsorption results of nanotubes before and after modification are shown in Tables 4 and 5.

It can be seen from the table that the adsorption capacity of nanotubes before and after modification increases with the increase of adsorption time. When the adsorption time is 90 minutes, the adsorption capacity of nanotubes before modification is 6.27mg/g, and the adsorption capacity of nanotubes after modification is 9.28mg/g. At this time, the adsorption capacity of nanotubes after modification is more than that before modification. 3.00mg/g. The relationship between removal rate and adsorption time is shown in Figure 5 (right) below.

It can be seen from the results in the figure that the removal rate of Zn2+ by the nanotubes before and after the modification increases with the increase of the adsorption time. The time for adsorption to reach equilibrium is 90 minutes, and the removal rates of nanotubes before and after modification are 42% and 69%, respectively; the adsorption time is within 30min-60min. The adsorption rate of nanotubes to Zn2+ before and after modification is very fast. At this time, the removal rate of nanotubes after modification is up to 20% higher than that before modification.

Table 4. The relationship between adsorption of Zn2+ by nanotubes and time before modification

Time (min)	Absorbance	The amount of Cu^{2+} (ug)	Cu^{2+} initial concentration (mg/L)	Concentration of Cu^{2+} (mg/L)	Adsorption capacity	Heavy metal ion removal rate
20	0.899	11.2983	1	2.3562	2.7213	18.1312
40	0.698	8.7953	1	1.7839	5.4397	35.8921
60	0.643	7.9321	1	1.6538	6.2782	40.3321
80	0.643	7.9321	1	1.6532	6.2782	40.3321

Table 5. The relationship between the adsorption of Zn2+ by the modified nanotubes and the time

Time (min)	Absorbance	The amount of Cu^{2+} (ug)	Cu^{2+} initial concentration (mg/L)	Concentration of Cu^{2+} (mg/L)	Adsorption capacity	Heavy metal ion removal rate
20	0.693	9.3278	1	1.9862	4.6321	29.6732
40	0.474	5.7865	1	1.2653	8.3872	53.8792
60	0.285	3.9868	1	0.8923	9.2871	65.8721
80	0.285	3.9868	1	0.8923	9.2871	65.8721

3.4. Garden Stone Carving Design Based on Nano-Materials

Due to the wear resistance of the modified surface of nano-materials, it has extraordinary significance in stone carving design. The status of stone carvings in each historical period is changing, and their biggest change was in the 20th century. When stone sculpture suddenly breaks the traditional norms and moves towards a public garden environment completely independent of

the dispensable, it becomes difficult to manage. But stone carving is still a spiritual creation of human beings. It exists in the garden as a kind of education and occupies an independent form of garden space. The important thing is, in more cases, where and in what form it will appear. Stone carving is not a work of art required by natural landscapes, but the blessings of people who need the natural environment. It needs the complete protection of people and the perfection of art. Landscape art will once again expand the field of sculpture. Obviously, the design of stone sculptures can already be extended to a broader field, and the application of all possible forms is achievable. Stone carvings are of great significance to the design of public gardens. The natural integration of stone carvings and gardens, their design, and their affinity with people may be practical issues in modern garden landscapes. In the past era, people can see sacred stone sculptures as idols, as accompanying stone sculptures, symbolizing the human spirit, as pure artistic sculptures, like thought stone sculptures, have evolved into an irresistible mixture. In these thoughts about the continuous advancement of sculpture art, almost all art forms in the past have been exhausted, and perhaps in a long period of time, various parallel forms will appear. Generally speaking, the size of artistic stone carving should be used as a point in the art form of the garden under the overall planning and construction of the park landscape. As well as a small part of urban planning or square landscape, but it has never been lacking like the human eye-it can let the soul pass through. It is undisputed that landscape sculpture exists in the field of landscape environment and landscape art. Its development must conform to the spiritual orientation of society and mankind. In accordance with the times, things will be printed in all fields, so that the concept of landscape art and sculpture art always keeps pace with the times. In the future, the development of folk sculpture art still depends on the in-depth thinking of folk artists and the intensive processing of works. However, with the cooperation of the garden designer and creating appropriate conditions, the garden sculptures in the garden must be unusually open. In order to improve the application level of sculptures in the landscape, take sculpture as a work of art in the garden landscape and make it to a perfect boundary, thereby improving the artistic level of landscape construction. Figure 6 shows the stone carving art based on nano wear resistance.

Figure 6. Stone carving art based on nano wear resistance

The sculpture art works in the garden generally constitute the main body and visual center of the specific landscape of the garden. In terms of folk aesthetics, spatial configuration, scale, color quality, etc., coordinate with the environment to form the internal elements of the park and the overall humanistic environment. Sculpture art in modern gardens is not a specific art form, nor does

it require a single style. It is a way of thinking that allows the artistic atmosphere to exist in the garden space. Keeping in touch with the public in the sense of modern culture, and the spirit and attitude of opening and communicating garden space are also the value orientation of garden space sculpture art. Therefore, sculpture art and landscape have broad and brilliant prospects.

4. Discuss

With the rapid development of social economy and urban construction, garden sculpture, as an indispensable element of art and culture in the public space environment, has become an important symbol of the level of urban cultural development. Sculptures are like eyes in the environment, conveying elegance and charm. They are an organic part of the garden landscape and are integrated with the garden landscape. The garden sculpture naturally divides the space, enhances the sense of hierarchy and layering of the garden space, and reflects the level of garden art and cultural taste. Culture is not only a concentrated historical culture, but also a flowing spiritual sustenance. Its pursuit of artistic beauty, yearning for garden nature and great artistic charm all reflect the beauty of garden sculptures. To organically combine the concepts of garden sculpture with those of garden designers, it is necessary to let people embrace art, fully release the vision of embracing nature, and let the infinite mass art and popular customs of the world be inherited and continued in garden sculptures. We need to inherit the past, respect the general trend of the garden industry, create classical art landscape sculptures, inject strong spiritual power into the landscape, make the landscape space reach the perceptual spirit and artistic charm, improve the overall cultural awareness of the landscape, and improve the level of landscape art. We are optimistic that in the near future, due to the prosperity of popular art, the level of landscape architecture will be improved, and new landscape art belonging to this area will be created.

5. Conclusion

In this paper, the influence of SiO2 nano content in the PPS-PTFE/SiO2 composite coating on the wear resistance and corrosion resistance of the coating was studied. After rubbing for 8m on sandpaper, the contact angle of the PPS-PTFE/0.08gSiO2 composite coating has the smallest change before and after rubbing. In addition, the corrosion potential of the PPS-PTFE/SiO2 composite coating is larger than that of the aluminum alloy substrate, and the corrosion resistance is better. At the same time, the adsorption rate of heavy metal ions was studied based on the nano surface modification of powder metallurgy parts. When the nanotubes removed Cu2+, Zn2+, and plasma before and after the modification, the time to reach the adsorption equilibrium was different. The adsorption equilibrium time for Cu2+ adsorption is 90min; the adsorption equilibrium time for Zn2+ adsorption is 90min. After the adsorption reaches the adsorption equilibrium, the removal rate of the nanotubes before and after the modification does not change. At this time, the removal rate of the nanotubes after the modification is higher than that before the modification. The removal rate of Cu2+ and Zn2+ plasma by nanotubes before and after modification increases with the increase of the concentration of the ion solution, and the removal rate of nanotubes after modification is greater than that before modification. When the Cu2+ solution concentration range is 1mg/L~3mg/L, the removal rate of nanotubes after modification is up to 11% higher than that before modification; When the concentration of Zn2+ solution ranged from 1 mg/L to 5 mg/L, the removal rate of nanotubes after modification was increased by up to 20% compared with that before modification.

Funding

This article is not supported by any foundation.

Data Availability

Data sharing is not applicable to this article as no new data were created or analysed in this study.

Conflict of Interest

The author states that this article has no conflict of interest.

References

[1] Brzhozovskii B M, Zinina E P, Martynov V V, et al. Wear resistance of cutting tools with a plasma-modified surface layer. Russian Engineering Research. (2017) 37(10): 882-887. https://doi.org/10.3103/S1068798X17100069

[2] Stepankin I N, Pozdnyako V E P, Kuis D V. Contact Wear of X165GrMoV12 and X160GrMoV12-1 Moderate Heat Resistant Die Steels with a Surface Modified Layer. Journal of Friction and Wear. (2019) 40(1): 1-5. https://doi.org/10.3103/S1068366619010173

[3] Ivanov Y F, Klopotov A A, EA Petrikova, et al. Surface of high-chromium steel modified by an intense pulsed electron beam. Steel in Translation. (2017) 47(10): 669-674. https://doi.org/10.3103/S0967091217100047

[4] Tsyganov V V, Mok H Nach R E, Sheiko S P. Increasing Wear Resistance of Steel by Optimizing Structural State of Surface Layer. Steel in Translation. (2021) 51(2): 144-147. https://doi.org/10.3103/S096709122102011X

[5] Wang Z G, Ouyang J H, Ma Y H, et al. Grain size dependence, mechanical properties and surface nanoeutectic modification of Al2O3-ZrO2 ceramic. Ceramics International. (2019) 45(11): 14297-14304. https://doi.org/10.1016/j.ceramint.2019.04.140

[6] Zagulyaev D V, Gromov V E, Konovalov S V, et al. Increase in Wear Resistance of the Surface Layers of AK10M2N Silumin at Electron-Beam Treatment. Inorganic Materials: Applied Research. (2019) 10(3): 622-628. https://doi.org/10.1134/S2075113319030432

[7] Potekaev A I, Ivanov Y F, Klopotov A A, et al. Structural-Phase State and Properties of Steel After Plasma-Electron Modification. Russian Physics Journal. (2019) 62(6): 940-947. https://doi.org/10.1007/s11182-019-01799-5

[8] Ning Z, Li T, Hui G, et al. Microstructure and Wear Resistance of Laser Cladded Ni-based Coatings with Nanometer La2O3 Addition. Rare Metal Materials & Engineering. (2017) 46(8): 2092-2096. https://doi.org/10.1016/S1875-5372(17)30185-6

[9] Mao X, Sun J, Zhou X, et al. Effect of Annealing Temperature on Surface Gradient Fine Microstructure and Wear Resistance of Low-Carbon Steel. Journal of Materials Engineering and Performance. (2020) 29(10): 6952-6959. https://doi.org/10.1007/s11665-020-05129-6

[10] Song W, Xu X, Liu S, et al. Effect on the Wear Resistance of Copper Alloy Surface Modification Layer by FSSP Implanting W Particles. Materials Transactions. (2019) 60(5): 765-769. https://doi.org/10.2320/matertrans.M2018316

[11] Marani, Saeed, Mehrang. Investigating Nano-Coated Surfaces in Improvement Wear Resistance of Tillage Tools. Emirates Journal for Engineering Research. (2019) 25(1): 5-5.

[12] Wojda S M, Sajewicz E. Influence of dental materials on hardness and Young's modulus of the surface layers of tooth enamel formed as a result of friction. Acta of bioengineering and biomechanics / Wroclaw University of Technology. (2019) 21(1): 129-139.

[13] Kudryashov A E, Zamulaeva E I, Levashov E A, et al. Application of Electrospark Deposition and Modified SHS Electrode Materials to Improve the Endurance of Hot Mill Rolls. Part 2.

Structure and Properties of the Formed Coatings. Surface Engineering and Applied Electrochemistry. (2019) 55(5): 502-513. https://doi.org/10.3103/S1068375519050089

[14] Dan, Rea. Digital Craftsmanship in Stone Design. The construction specifier. (2017) 70(5): 84-88.

[15] Kelso J. Specifying Stone Composite Panels. The Construction Specifier. (2019) 72(4): 40-44.

[16] Stone, Tracy, A, et al. Therapeutic design of peptide modulators of protein-protein interactions in membranes. Biochimica et biophysica acta. Biomembranes. (2017) 1859(4): 577-585. https://doi.org/10.1016/j.bbamem.2016.08.013

[17] Fadin V V, Aleutdinova M I. Wear Resistance of Carbon Steels and Structure Parameters of Their Surface Layer After High Current Density Sliding. Russian Physics Journal. (2016) 58(12): 1726-1731. https://doi.org/10.1007/s11182-016-0708-9

[18] Ovcharenko V E, Ivanov Y F, Mohovikov A A, et al. Wear resistance of the surface layers of hard alloys with a multilevel structural phase state. Journal of Surface Investigation X-ray Synchrotron and Neutron Techniques. (2016) 10(4): 718-722. https://doi.org/10.1134/S1027451016040145

[19] Romanov D A, Protopopov E V. Effect of Electron-Beam Treatment on Wear-Resistant Coatings Applied by Electroexplosive Sputtering. Steel in Translation. (2017) 47(12): 782-787. https://doi.org/10.3103/S0967091217120105

[20] Lei Y S, Yan H, Wei Z F, et al. Effect of hot extrusion on microstructure and tribological behavior of Al2O3p reinforced 7075 aluminum-matrix composites. Journal of Central South University. (2021) 28(8): 2269-2284. https://doi.org/10.1007/s11771-021-4768-9

[21] Li J, Zhang Q, Chen Z. Aggregate Shape Analysis and Evaluation of Modified Epoxy Wear Layer for Cement Pavement. Shenyang Jianzhu Daxue Xuebao (Ziran Kexue Ban)/Journal of Shenyang Jianzhu University (Natural Science). (2017) 33(6): 1055-1064.

[22] Sedykh L V, Borisov P V, Pashkov A N, et al. Development of flotation machine impeller on the base of additive technologies. Izvestiya Vysshikh Uchebnykh Zavedenij. Chernaya Metallurgiya. (2021) 64(5): 366-373. https://doi.org/10.17073/0368-0797-2021-5-366-373

[23] Kochetkova A S, Gorbushin P N, Sosnov E A, et al. Scanning probe microscopy estimation of the wear resistance of the surface of a modified PVC film. Russian Metallurgy. (2017) 2017(4): 312-318. https://doi.org/10.1134/S0036029517040097

[24] Vinokurov E G, Zuev K V, Zhigunov F N, et al. Wear Resistance of Nickel-Phosphorus-Modified Copper Phthalocyanate Composition Coatings. Protection of Metals & Physical Chemistry of Surfaces. (2018) 54(1): 92-94. https://doi.org/10.1134/S2070205118010136

[25] Feng Z, Liang W, Tao D, et al. CU-Net: Component Unmixing Network for Textile Fiber Identification. International Journal of Computer Vision. (2019) 127(10): 1443-1454. https://doi.org/10.1007/s11263-019-01199-9